Range and stability of structural colors generated by *Morpho*-inspired color reflectors

Kyungjae Chung[1] and Jung H. Shin[1,2,*]

[1]*Department of Physics, KAIST, 335 Gwahak-ro, Yuseong-Gu, Daejeon 305-701, South Korea*
[2]*Graduate School of Nanoscience and Technology (WCU), KAIST, 335 Gwahak-ro, Yuseong-Gu, Daejeon 305-701, South Korea*
**Corresponding author: jhs@kaist.ac.kr*

Received January 29, 2013; revised March 22, 2013; accepted March 22, 2013;
posted March 22, 2013 (Doc. ID 184338); published April 23, 2013

The range and stability of structural colors generated by *Morpho*-inspired color reflectors are investigated. We find that despite the internal randomness of such structures that gives rise to their *Morpho*-like angle-independent iridescence, their colors under ambient lighting condition can be predicted by simple transfer-matrix calculations of corresponding planar multilayer structures. By calculating the possible range of colors generated by multilayers of different structures and material combinations using such transfer-matrix methods, we find that low-refractive index multilayers with intrastructure absorption, such as the melanin-containing chitin/air multilayer structure from the *Morpho* butterflies, can provide not only the most pure structural colors with the largest color gamut, but also the highest stability of color against variations in multilayer structure.

OCIS codes: (330.1690) Color; (330.1710) Color, measurement.
http://dx.doi.org/10.1364/JOSAA.30.000962

1. INTRODUCTION

Structural colors that arise due to reflection and interference of light from periodic structures form the basis for some of the most dazzling displays of color in nature [1–4]. They can be much brighter than pigment-based colors, and share the common characteristics of intricate changes in color with changing viewing angles. Yet *Morpho* butterflies, which are arguably one of the most widely cited examples of structural color, are characterized by the fact that their color appears blue over a wide range of viewing angles [5]. This paradox has long been the subject of many scientific investigations [6–8], and by now, many have reported that while the multilayered ridges on the scales of *Morpho* butterflies are responsible for the color, the narrow, tapering shape of the ridges, together with the small, random variations in their structure, shape, and location, remove coherence among different ridges, and give rise to further optical effects, such as diffraction and scattering that result in the bright, yet angle-independent iridescence [7].

At the same time, such complexity has made both reproducing and investigating the optical properties of the structures difficult. Consequently, previous investigations used complex, time-consuming methods, such as ion beam chemical deposition [9] or finite-difference time-domain (FDTD) simulations [10–12], which can limit the scope of investigations. Recently, using simple multilayer deposition on a silica microsphere substrate, we successfully fabricated large-scale, flexible color reflectors that reproduce the bright, angle-independent iridescence of *Morpho* butterflies [13], and provide potential for a wide range of applications, such as reflective displays, sensors [14,15], and fashion. In this paper, we investigate and compare the range and stability of structural colors that can be generated by such *Morpho*-inspired color reflectors with those expected of *Morpho* butterflies. We find that despite the internal disorder, the color of such a structure under ambient light conditions is closely matched by that of a conventional, flat multilayer having the same periodicity when viewed normally. This enables us to use simple transfer-matrix method (TMM) calculations to scan a wide range of materials and structures for their color. The results indicate that the chitin/air multilayer structure of *Morpho* butterflies can produce a larger color gamut with purer colors that are most stable than the dielectric-based multilayers can, aided in part by their low refractive indices, and also by the strong absorption within the chitin layers.

2. METHOD

Morpho-inspired color reflectors were fabricated by depositing TiO_2/SiO_2 multilayers on a monolayer of silica microspheres with diameters ranging from 200 to 400 nm using low-pressure, directional sputter deposition. Prior to the deposition of the multilayers, a 300 nm thick Cr layer was deposited to provide a black, absorbing background. The directionality of the deposition process preserves the shape of the underlying silica microspheres, resulting in a thin film that is comprised of multilayer columns of identical periodicity but with random variations in spatial location, and thus replicates the internal disorder of *Morpho* butterfly wing scales. Scanning electron microscope (SEM) images of a typical multilayer thin film are shown in Fig. 1. Also shown are the SEM images of a dorsal scale from a *Morpho rhetenor* butterfly, showing the lamella-structured ridges that give rise to its color. For comparison, a flat multilayer film was also deposited concurrently on a Si wafer. Detailed description of the deposition process and the film can be found in [13].

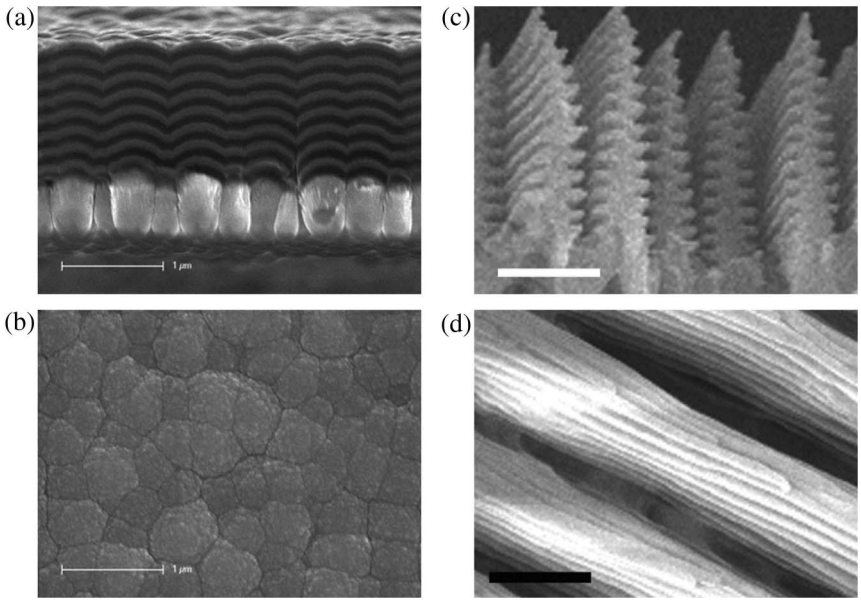

Fig. 1. (a) SEM images of *Morpho*-inspired film in cross-sectional view. The dark bands are TiO_2 layers and the light bands are the SiO_2 layers. SiO_2 microspheres and the Cr absorption layers can be seen as well. Note the random wiggling of the layers that reflects the diameter variation of the underlying silica microspheres. (b) The same film seen in top view. The tile-like shape reflects the diameters of the underlying silica microspheres. (c) Lamella-structured ridges in dorsal scale of actual *Morpho rhetenor* butterfly in cross-sectional view. (d) Dorsal scale in top view. Scale bars in (c) and (d) are 1 μm.

The reflectance spectra of the deposited films were measured in two ways. First, normal reflectance spectra under ambient lighting conditions were obtained using a DMS 505 made by Autronic. The equipment provides a hemisphere of diffuse, white light, and is a standard method of evaluating flat-panel displays as it closely resembles lighting condition of living space. Second, specular reflectance spectra in the normal direction under collimated light illumination were obtained using a conventional spectrometer. In all cases, the reflectance values were normalized against a reflectance standard (Avantes RS-2).

TMM calculations were performed on eight-pair multilayers of TiO_2/SiO_2, SiO_2/Si, Si_3N_4/SiO_2, and TiO_2/Si_3N_4. These materials were chosen for their compatibility with standard thin-film deposition processes and wide range of refractive indices. Eight-pair multilayers were chosen as further increase in the number of layers did not result in any significant change in reflectance (data not shown). For comparison, TMM calculations chitin/air multilayer with complex refractive indices as reported for *Morpho* butterflies [16] were also performed. In all cases, a wavelength region from 360 to 830 nm was considered, and a perfectly black bottom layer to absorb any transmitted light was included. For each material combination, the layer thicknesses were varied from 30 to 250 nm in 5 nm increments for both low-index and high-index layers, for a total of 2025 combinations of layer thicknesses. The real and imaginary parts of the refractive indices used in calculations are summarized below in Fig. 2.

For color comparisons, the reflectance spectra were converted into coordinate information in color space using color matching function of CIE 1931 2° Standard Observer. The ranges of possible colors were analyzed using the National Television System Committee (NTSC) parameters.

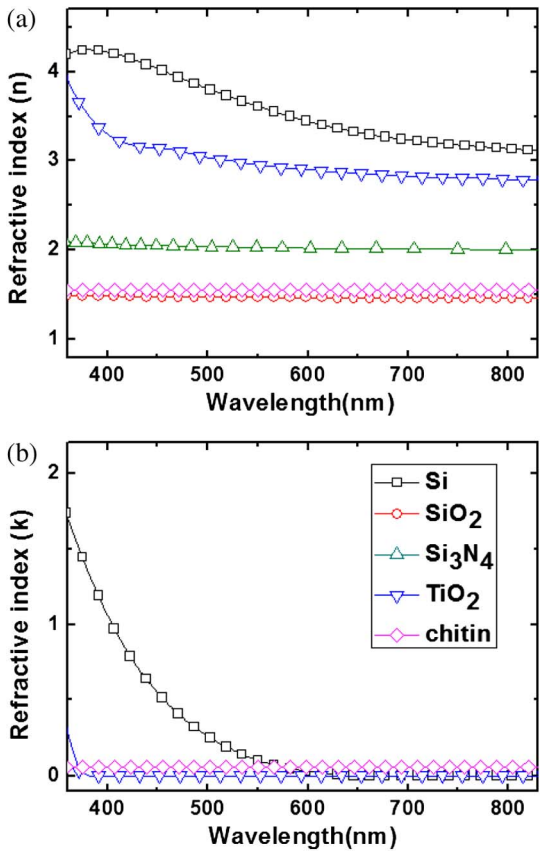

Fig. 2. (a) Real part and (b) imaginary part of refractive indices of materials used in TMM calculation. Absorption by Si_3N_4 and SiO_2 is taken to be zero at all wavelength ranges. The values for chitin were taken from [16]. Note that chitin has nonzero absorption across the entire visible range.

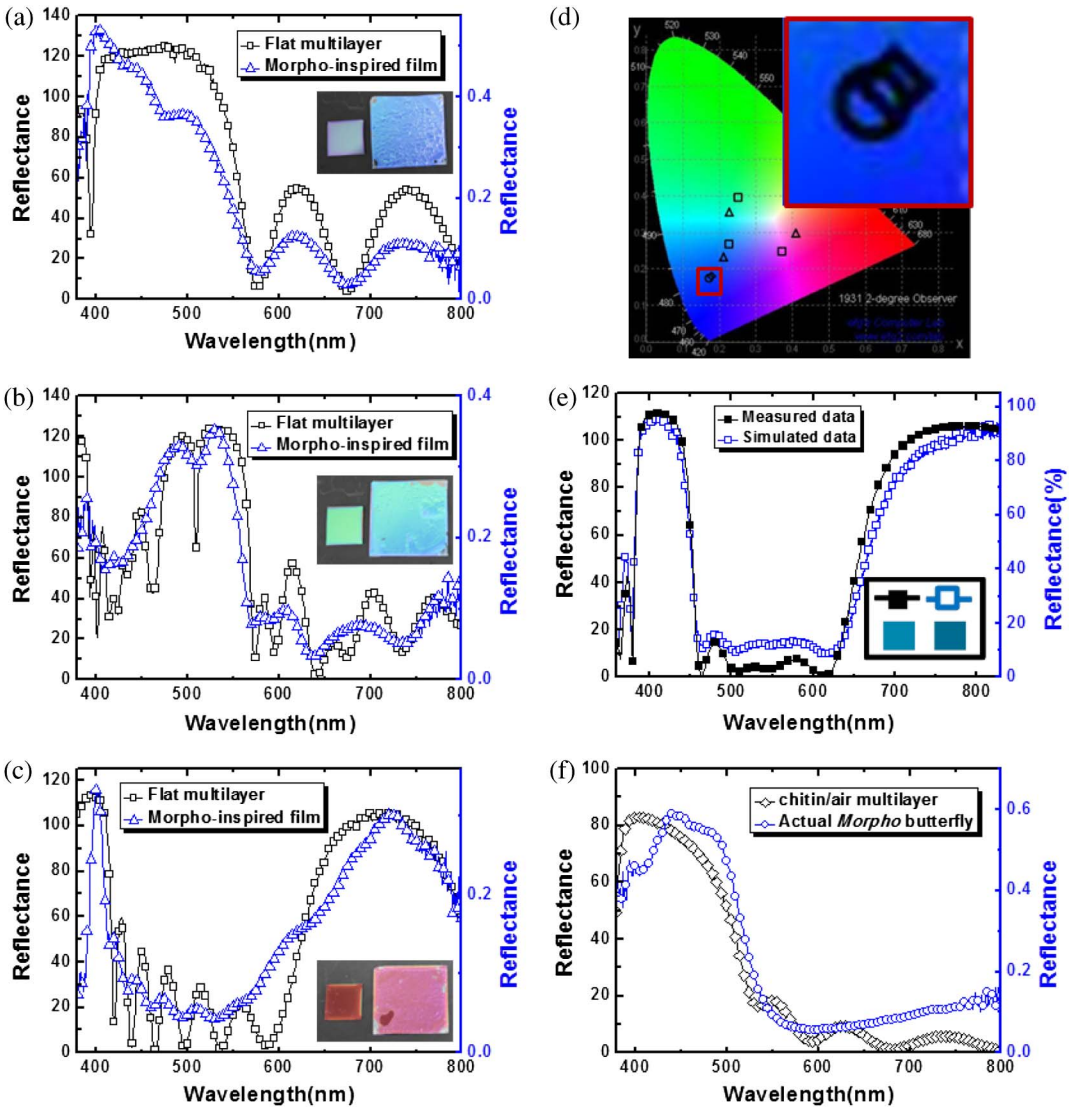

Fig. 3. Reflectance spectra of (a) blue, (b) green, and (c) red *Morpho*-inspired thin films, measured by DMS 505 under ambient lighting conditions, and reflectance spectra of corresponding flat, multilayer thin films, measured by a spectrometer under normal illumination. The inset shows the optical images of the films. In all cases, the one on the left is the flat multilayer thin film, and the one on the right is the *Morpho*-inspired thin film. Note that the measured reflectance from flat multilayer thin films exceeds 100% at some wavelengths. This is an artifact of the normalization process, and should be taken to indicate a very high reflectance of near 100%. (d) The colors corresponding to the measured and reflectance spectra, shown as coordinates on the 1931 CIE diagram. In inset, color space including measured data of actual *Morpho* butterfly shown in (f) is magnified. Icons are overlapped because two colors are too close. (e) Comparison of the measured and TMM-calculated reflectance spectra of a flat multilayer thin film. The inset indicates corresponding colors to the reflectance spectra. (f) Reflectance spectra of actual *Morpho rhetenor* butterfly measured by DMS 505, and reflectance spectra of chitin/air multilayer. The thickness of chitin/air multilayer is obtained and averaged from Fig. 1(c).

3. RESULTS

The measured reflectance spectra from both *Morpho*-inspired color reflectors and corresponding flat multilayer thin films are shown in Figs. 3(a)–3(c), respectively. The inset shows the optical images of the films. The *Morpho*-inspired films show lower specular reflectance due to scattering. Note that the measured reflectance from flat multilayer thin films exceeds 100% at some wavelengths. This is an artifact of the normalization process, and should be taken to indicate a very high reflectance of near 100%. However, we find that despite the differences in the structure and the lighting condition, the normal reflectance spectra of *Morpho*-inspired thin films under ambient light conditions are similar to those of corresponding flat multilayers under specular reflection conditions. In particular, while the sharpness of many of the features is washed out, the location of reflectance maxima and minima, and the relative height of the reflectance maxima are comparable to each other. Consequently, the colors of the films, both to the eye as shown in the inset, and as determined by coordinates on the CIE diagram as is shown in Fig. 3(d), agree closely.

We note that such an agreement is valid for normal incidence only, since only the *Morpho*-inspired thin films retain their color as the viewing angle changes. At the same time, this angle-independence also means that the color of a *Morpho*-inspired thin films, which can be quite difficult to calculate due to the internal complexity of the film even under specular reflection let alone under ambient lighting condition, can be predicted by the color of a flat multilayer under

normal, specular reflection. But the reflectance, and therefore the color, or such a flat multilayer film can be easily and accurately calculated using simple TMM, as shown in Fig. 3(e). Thus, the results in Fig. 3 indicate that to simply predict the range of colors that are available from such *Morpho*-inspired thin films we may use simple TMM calculations instead of complex simulations such as FDTD.

In case of natural *Morpho* butterflies, there exist strong intra- and inter-ridge variations in the layer spacings. Still, as Fig. 3(f) shows, the reflectance spectrum from a TMM simulation using the average spacing obtained from Fig. 1(c) is comparable to the normal reflectance spectrum of an actual *Morpho rhetenor* butterfly under ambient light conditions. More importantly, the color predicted by a TMM simulation agrees well with that from a natural *Morpho* butterfly, as is shown in Fig. 3(d), indicating that such simulation approach may work with natural *Morpho* butterflies as well.

Figures 4(a)–4(e) show the results of TMM calculations on the possible range of colors from SiO_2/Si, TiO_2/SiO_2, TiO_2/Si_3N_4, Si_3N_4/SiO_2, and chitin/air multilayers, respectively. Each dot represents a particular combination of low-index/high-index layer thicknesses, for a total of 2025 combinations. The largest possible color gamut, obtained by taking the best blue, green, and red colors as determined by distance from points corresponding to wavelength 450, 520, and 680 nm in border line of CIE 1931 color diagram, is indicated by the triangle, with the values given in Table 1. We find that the possible range of colors depends strongly on the material used. The SiO_2/Si multilayers give the smallest color gamut of 36%, while the TiO_2/SiO_2 multilayers, which were used to fabricate *Morpho*-mimetic structures, provide a color gamut of only 55%. The highest value is obtained from the chitin/air multilayers, which provide a color gamut of 80%.

One obvious reason for such difference in the color gamut is the difference in the index contrast. As shown in Figs. 4(f)–4(j), the lower index contrast results in narrower stop-gap responsible for the main reflection peak, resulting in purer colors. However, the fact that the Si_3N_4/SiO_2

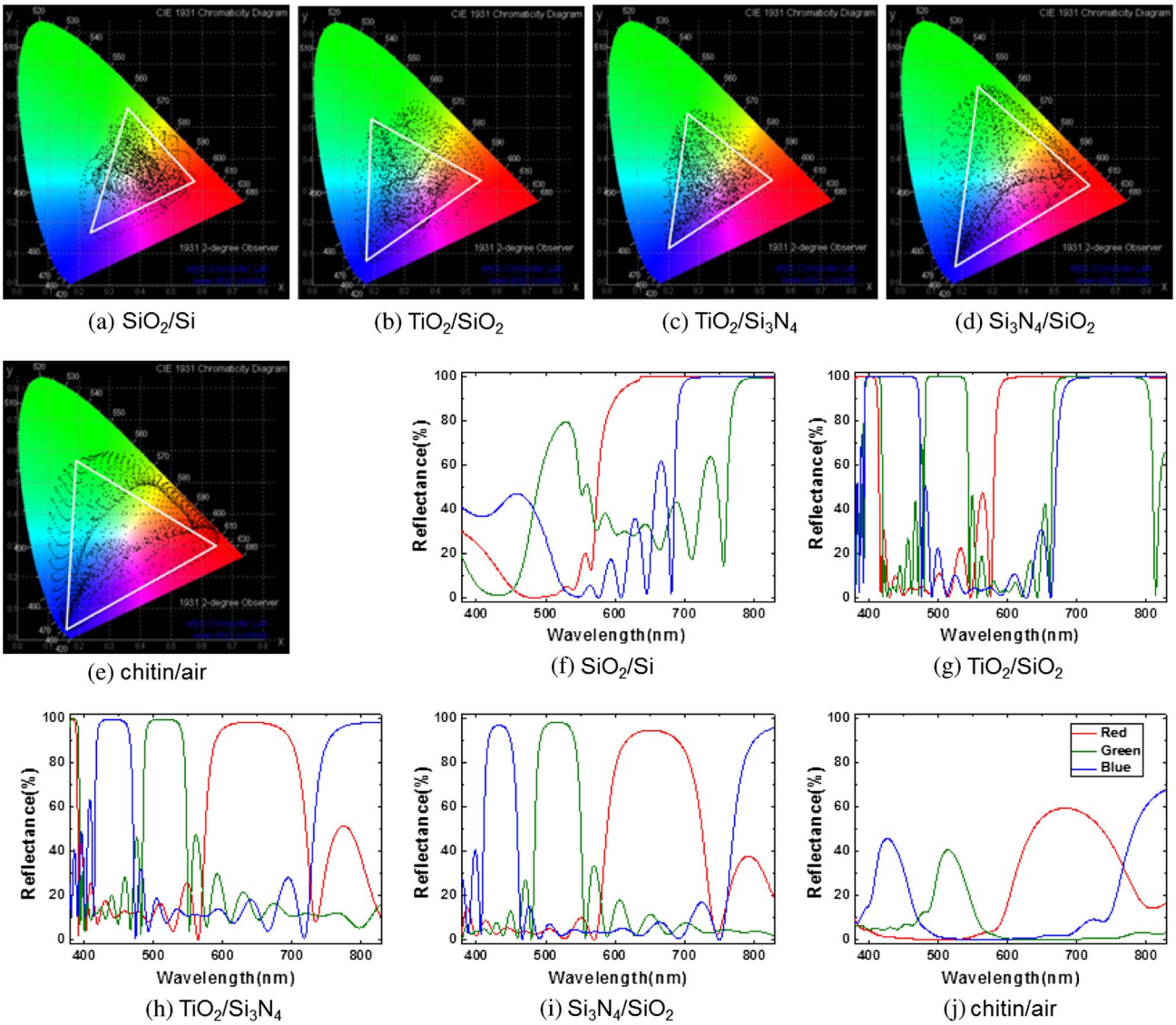

Fig. 4. Range of colors possible from (a) SiO_2/Si, (b) TiO_2/SiO_2, (c) TiO_2/Si_3N_4, (d) Si_3N_4/SiO_2, and (e) chitin/air multilayers, as predicted by TMM calculations. The largest possible color gamut from each multilayer combination is indicated by the triangle. (f)–(j) The calculated reflectance spectra from the selected blue, green, and red points that provide the largest color gamut. The layer thicknesses are shown in Table 1.

Table 1. Layer Thicknesses of the Red, Green, and Blue Points for Largest Color Gamut[a]

	Red	Green	Blue	Gamut (%)
SiO_2/Si	85/65	210/50	115/80	36
TiO_2/SiO_2	75/90	205/100	95/85	55
TiO_2/Si_3N_4	75/50	130/60	95/70	39
Si_3N_4/SiO_2	115/60	195/80	140/100	67
Chitin/air	160/85	205/205	180/155	80

[a]Unit of layer thicknesses is nanometer.

multilayers, whose refractive index contrast of $\Delta n = 0.60$–0.54 matches that of chitin/air multilayer ($\Delta n = 0.56$) very closely, still provides a smaller color gamut indicates that for obtaining pure colors and large color gamut, the absolute values of refractive indices need to be low as well. Indeed, TiO_2/SiO_2 multilayers have a larger color gamut than TiO_2/Si_3N_4 multilayers despite the larger refractive index contrast.

It must be noted here that the reflectance peaks of chitin/air multilayers are lower, and have a more rounded shape. This is due to absorption within the chitin layers by the pigment melanin that is strong enough to turn the scale nearly opaque [17]. If we assume a pure chitin layer such that the absorption in the visible range is negligible [18], then the maximum reflectance approaches 100%, with concomitant increase of the color gamut to 92% (data not shown). However, optical absorption within the chitin layer plays another important role as well, as will be discussed later.

In all calculations so far, we assumed a multilayer of perfect periodicity. Such a perfect periodicity, however, is very difficult to achieve even in a controlled laboratory setting, let alone inside the scales of *Morpho* butterflies which arise spontaneously during the growth of the scales [19]. Thus, we have investigated the effect of such error in the periodic structure on the structural color by assigning a thickness variation of 5 nm such that the layer thickness can differ from the intended value by +5, 0, or −5 nm. It is repeated for all five-pair layers for a total of $3^{10} = 59{,}049$ combinations of layer thicknesses. The number of layers in this calculation was reduced to five-pair from eight-pair due to the inordinate amount of time required to simulate the $3^{16} = 43$ million combinations. Such errors in periodicity can also give an insight into the angle

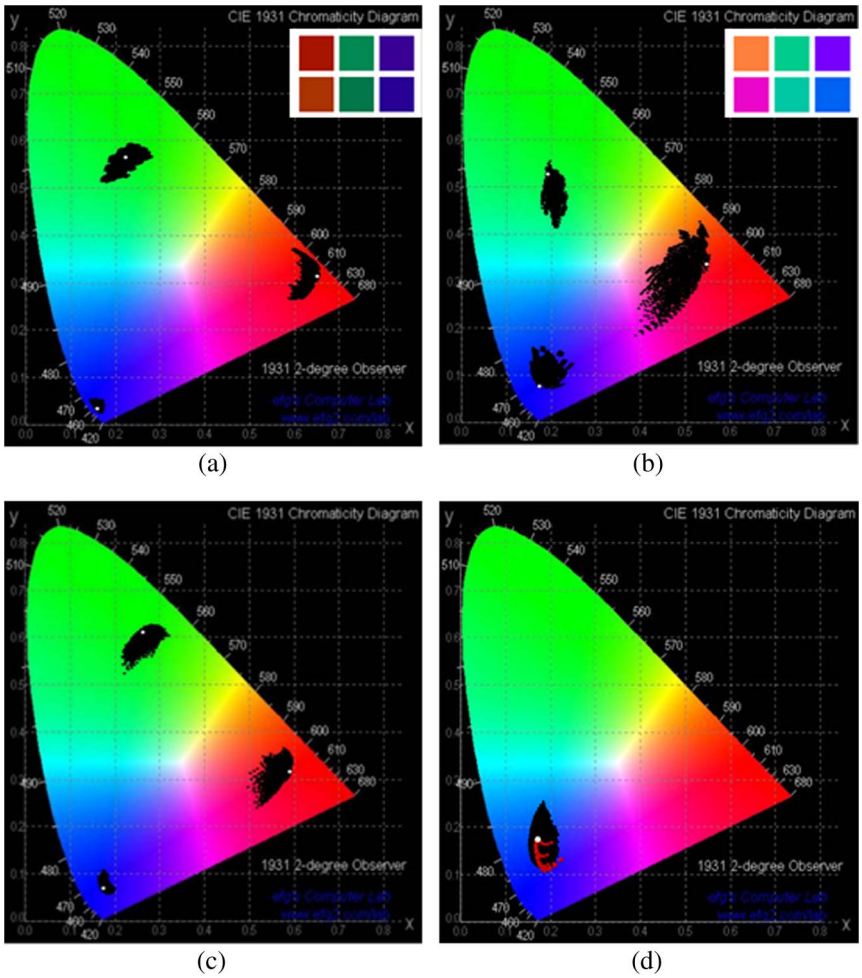

Fig. 5. TMM calculated results of simulating errors of 5 nm in the layer thickness on the colors of the multilayers. White point indicates the optimal colors from Fig. 4, and black area is made of densely overlapped, 59 thousand points, resulting from 5 nm variation in each layer thicknesses. (a) Chitin/air, (b) TiO_2/SiO_2, and (c) Si_3N_4/SiO_2 results. The insets show the colors of the three optimum points in the upper row, and the colors of points farthest away from the optimum points in the bottom row. (d) The result of simulating errors of 5 nm in the layer thickness for a *Morpho rhetenor* butterfly. White point is the color of real *Morpho rhetenor* butterfly, and red points show the measured color shift of *Morpho rhetenor* upon changing viewing angle under ambient light condition.

Table 2. Calculated ΔE in Lab System between the Optimum Points and Farthest Points of Fig. 5

	Red	Green	Blue
Chitin/air	9.78	6.46	30.25
TiO_2/SiO_2	107.67	29.26	84.50
Si_3N_4/SiO_2	21.61	17.09	38.03
Chitin/air (no absorption)	25.63	21.58	38.37

dependence of the structural colors, as changing the viewing angle is equivalent to changing the effective periodicity of the multilayer.

The results of this investigation are summarized in Fig. 5. Figures 5(a)–5(c) show the results introducing the 5 nm error to chitin/air, TiO_2/SiO_2, and Si_3N_4/SiO_2 multilayers that were optimized for maximum color gamut, respectively. Again, we find strong dependence on the materials used. The TiO_2/SiO_2 multilayer structure shows the strongest change in colors such that the orange-red color of optimum film changes to pink/purple even though the layer thicknesses are changed from 75/90 to 70/85 nm only, while the chitin/air and Si_3N_4/SiO_2 multilayers show much smaller color changes. Figure 5(d) shows the result of introducing variations in thickness to a chitin/air multilayer whose dimension and color agree with those from an actual *Morpho rhetenor* butterfly. Interestingly, we find that the experimentally obtained, angle-dependent changes in color from the same butterfly lie well within the theoretically predicted range, indicating that, indeed, these calculations may be used to predict the range of angle-dependent color variation in *Morpho*-inspired structures.

However, distances on a CIE 1931 color plot do not necessarily correspond to differences in perceived color. Thus, for a more quantitative comparison of color stability, we use the color distance metric ΔE, calculated by transforming the data shown in Fig. 5 using the 1976 Lab system [20]. ΔE is a value used to estimate color difference that takes under consideration the hue, saturation, brightness, and even human's perception. Typically, a ΔE value of 2.3 is taken to be the just noticeable to the human eye [20]. The values of ΔE between the optimum point (shown as white dots in Fig. 5) and the point farthest away from such optimum point are summarized in Table 2.

We find that the chitin/air multilayer, which provides the largest color gamut, has the lowest value of ΔE, indicating the highest color stability, for all colors as well. One major reason for such stability is the optical absorption within the chitin layers. As shown in the last row of Table 2, chitin/air multilayer shows values of ΔE that are much larger, and quite similar to that of Si_3N_4/SiO_2 multilayers, if we assume that chitin is pure such that it is transparent in the visible [18]. This is somewhat surprising, as we assume a perfectly black substrate for all films. The reason for such an advantage of optical absorption within the multilayer structure over an external absorption layer for color stability is not clear. It may be due to suppression of the weak sidebands to the main reflection peak by the intrinsic absorption, as can be seen in Fig. 4. The height and location of such sidebands are sensitive to errors in the layer thicknesses, and thus affect the perceived color. While more research is still needed for a more clear understanding, the results of Table 2 indicate that for best color stability, it would be better to introduce optical absorption within the reflecting multilayers directly instead of providing an external absorptive layer.

4. SUMMARY

In conclusion, we have investigated the range and stability of structural colors generated by *Morpho*-inspired color reflectors. We find that the color of *Morpho*-inspired color reflectors under ambient lighting conditions are quite similar to that of corresponding planar multilayer structures under normal illumination, even though only the *Morpho*-inspired color reflectors have the internal disorder necessary for angle-independent iridescence. This enables us to predict the range of colors possible by such structures using simple TMM calculations. Based on such calculations, we find that chitin/air multilayers as found on *Morpho* butterflies provide larger color gamut and better color stability against random structural variations than multilayers based on typical inorganic materials such as TiO_2 [21] and Al_2O_3 [22] that have been used so far, in part due to its lower refractive index, but also due to its intrastructure optical absorption. Based on the results, we suggest that multilayers based on low-index materials such as polymers or different glasses with built-in optical absorption would be optimal for creating the most pure, stable colors in a *Morpho*-inspired structure.

ACKNOWLEDGMENTS

This work was supported in part by the National Research Foundation of Korea (NRF) grant funded by the Korea government (MEST) (Grant Nos. 2010-0029255, K20815000003). J. H. Shin acknowledges support by WCU (World Class University) program through NRF of Korea funded by the Ministry of Education, Science and Technology, Grant No. R31-2008-000-10071-0.

REFERENCES

1. J. P. Vigneron and P. Simonis, *Advances in Insect Physiology* (Academic, 2010), Chap. 5.
2. C. W. Mason, "Structural colors in feathers," J. Phys. Chem. **27**, 202–251 (1923).
3. C. W. Mason, "Structural colors in insects," J. Phys. Chem. **30**, 383–395 (1926).
4. P. Vukusic and J. R. Samble, "Photonic structures in biology," Nature **424**, 852–855 (2003).
5. S. Yoshioka and S. Kinoshita, "Wavelength-selective and anisotropic light-diffusing scale on the wing of the *Morpho* butterfly," Proc. R. Soc. B **271**, 581–587 (2004).
6. S. Kinoshita, S. Yoshioka, and K. Kawagoe, "Mechanisms of structural colour in the *Morpho* butterfly: cooperation of regularity and irregularity in an iridescent scale," Proc. R. Soc. B **269**, 1417–1421 (2002).
7. S. Kinoshita, S. Yoshioka, Y. Fujii, and N. Okamoto, "Photophysics of structural color in the *Morpho* butterflies," Forma **17**, 103–121 (2002).
8. L. Plattner, "Optical properties of the scales of *Morpho rhetenor* butterflies: theoretical and experimental investigation of the back-scattering of light in the visible spectrum," J. R. Soc. Interface **1**, 49–59 (2004).
9. K. Watanabe, T. Hoshino, K. Kanda, Y. Haruyama, T. Kaito, and S. Matsui, "Optical measurement and fabrication from a *Morpho*-butterfly-scale quasistructure by focused ion beam chemical vapor deposition," J. Vac. Sci. Technol. B **23**, 570–574 (2005).
10. D. Zhu, S. Kinoshita, D. Cai, and J. B. Cole, "Investigation of structural colors in *Morpho* butterflies using the nonstandard-finite-difference time-domain method: effects of alternately

stacked shelves and ridge density," Phys. Rev. E **80**, 051924 (2009).
11. M. Kambe, D. Zhu, and S. Kinoshita, "Origin of retroreflection from a wing of the *Morpho* butterfly," J. Phys. Soc. Jpn. **80**, 054801 (2011).
12. A. Saito, M. Yonezawa, J. Murase, S. Juodkazis, V. Mizeikis, M. Akai-Kasaya, and Y. Kuwahara, "Numerical analysis on the optical role of nano-randomness on the *Morpho* butterfly's scale," J. Nanosci. Nanotechnol. **11**, 2785–2792 (2011).
13. K. Chung, S. Yu, C.-J. Heo, J. W. Shim, S.-M. Yang, M. G. Han, H.-S. Lee, Y. Jin, S. Y. Lee, N. Park, and J. H. Shin, "Flexible, angle-independent, structural color reflectors inspired by *Morpho* butterfly wings," Adv. Mater. **24**, 2375–2379 (2012).
14. R. A. Potyrailo, H. T. Ghiradella, A. Vertiatchikh, K. Dovidenko, J. R. Cournoyer, and E. Olson, "*Morpho* butterfly wing scales demonstrate highly selective vapour response," Nat. Photonics **1**, 123–128 (2007).
15. A. D. Pris, Y. Utturkar, C. Surman, W. G. Morris, A. Vert, S. Zalyubovskiy, T. Deng, H. T. Ghiradella, and R. A. Potyrailo, "Towards high-speed imaging of infrared photons with bio-inspired nanoarchitectures," Nat. Photonics **6**, 195–200 (2012).
16. P. Vukusic, J. R. Sambles, C. R. Lawrence, and R. J. Wootton, "Quantified interference and diffraction in single *Morpho* butterfly scales," Proc. R. Soc. B **266**, 1403–1411 (1999).
17. S. Zhang, X. Zhao, H. Xu, R. Zhu, and Z. Gu, "Fabrication of photonic crystals with nigrosine-doped poly(MMA-co-DVB-co-MMA) particles," J. Colloid Interface Sci. **316**, 168–174 (2007).
18. D. E. Azofeifa, H. J. Arguedas, and W. E. Vargars, "Optical properties of chitin and chitosan biopolymers with application to structural color analysis," Opt. Mater. **35**, 175–183 (2012).
19. H. Ghiradella, "Light and color on the wing: structural colors in butterflies and moths," Appl. Opt. **30**, 3492–3500 (1991).
20. G. Sharma, *Digital Color Imaging Handbook* (CRC, 2003), Chap. 1.
21. A. Saito, S. Yoshioka, and S. Kinoshita, "Reproduction of the *Morpho* butterfly's blue: arbitration of contradicting factors," Proc. SPIE **5526**, 188–194 (2004).
22. J. Huang, X. Wang, and Z. L. Wang, "Controlled replication of butterfly wings for achieving tunable photonic properties," Nano Lett. **6**, 2325–2331 (2006).